Neutral Hydrogen in External Galaxies

Arnold Rots

July 1 1975

For a topic like this there are two possible approaches : to consider one galaxy in considerable detail, or to consider just global parameters of many galaxies. Limited by resolution the second approach has been the prevailing one until recently. Now that detailed studies of galaxies other than Andromeda or the Magelanic Clouds are more or less available, it seems interesting to compare the two approaches. In doing so, it is surprising how the same parameters and the same problems are popping up. It turns out that the two methods are highly complementary and hence such a comparison is very clarifying and fruitful.

I would like to start out with the integral properties statistics on a relatively large number of galaxies. An excellent reference which I include in these notes to cover this subject is M. S. Roberts, 1974, Interstellar Hydrogen in Galaxies, Science 183, 371.

Then I would like to discuss one galaxy in detail : M 81, on the basis of Westerbork observations. This part is represented in these notes by a paper given at the CNRS symposium Dynamics of Spiral Galaxies (Paris 1974). Most of the figures of that paper are slightly outdated at present. This, however, does not affect the argument. Figs. 8^a and 8^b have been added. They contain M/L, B-V, and relative HI surface density as functions of radius.

Reprinted from
1 February 1974, Volume 183, pp. 371-378

SCIENCE

Interstellar Hydrogen in Galaxies

Radio observations of neutral hydrogen yield valuable information on the properties of galaxies.

Morton S. Roberts

In the past 20 years radio spectral line techniques have been used to study the interstellar hydrogen content of the nearer galaxies. These isolated systems of stars, gas, and dust typically have masses in the range 10^{43} to 10^{45} grams. They take second place on the mass scale to the physical groupings and clusters of galaxies which populate and define the universe.

The period during which the galaxies themselves have been recognized as separate entities rather than nebulous patches located within our "Milky Way universe" dates back only to 1924, when Hubble established that cepheid variable stars, a powerful astronomical yardstick, were present in the spiral nebula in Andromeda (*1*). He found that the nebula lay well beyond the confines of our own Milky Way system—the "island universe" theory was proved. An interesting and little-recognized sidelight was the derivation of a similarly large distance for the Andromeda galaxy by Opik a few years before Hubble's discovery of the cepheids (*2*). Opik employed a method commonly used today, that of assuming a constant ratio of mass to luminosity for galaxies. This assumption, together with rotation and luminosity information on Andromeda and a region in our own galaxy, enabled Opik to estimate the distance.

Developments of the following 30 years included recognition of different types of galaxies, the "Hubble types." The discovery that the distant galaxies are receding in a systematic manner proportional to their distance led to the velocity-distance correlation and the related Hubble constant, which gives the rate of expansion of the universe as well as a measure of its age. Galaxy counts were developed, but unsuccessfully applied, to derive the geometry of the universe. (Radio source counts are being used in similar analyses today with widely differing conclusions.)

The thrust of extragalactic research was aimed at cosmology. Little was known of the galaxies themselves. As basic a parameter as total mass was known for only a handful of galaxies. The gaseous interstellar component was only qualitatively described by the optical emission lines. Our understanding of the properties of galaxies was developing slowly because the necessary observational data were difficult to obtain: spectrographs were slow; photographic emulsions were slow; photoelectric techniques were in their infancy; the number of telescopes used for extragalactic studies were few; and, surprisingly, the number of astronomers working in this field were comparatively few.

The classification of galaxies by structural appearance seemed to offer important clues to our understanding of these systems. Some felt that it reflected an evolutionary sequence. But there was no agreement on which direction the evolution took. Figure 1 summarizes in a series of sketches the different galaxy types. Photographic examples are given in (*3–5*). There are two basic sequences: the ellipticals —which show no structural features, only different degrees of apparent flattening—and the spirals. The latter are further subdivided into regular and barred. In the regular systems the spiral arms come from the central nuclear region; the barred galaxies have their spiral structure starting from the ends of a central bar.

As a matter of convenience, the terms "early" and "late" are used to refer to the two ends of the sequence. Thus, S0's are earlier than Sb's, and irregular galaxies are late type systems. Hubble (*6*), in introducing this nomenclature, was careful to point out that no evolutionary or chronological significance was intended.

The classification of galaxies is a subjective procedure. The general features of the different types are well described, and one can quickly learn the classification scheme. But are there any physical parameters that can be associated with this subjective scheme? The color and the related quantity, the integrated spectral type, are usually well correlated with structural type. Another correlation, that of the ratio of total mass to luminosity, was suggested when relatively few galaxian masses were available (*7*). It does not appear to hold now, except for the broad subdivision of ellipticals and spirals, the former having a higher ratio by about an order of magnitude. No correlation among the various classes of spirals is indicated by the larger sample of mass determinations now available (*8*).

Hydrogen 21-Centimeter Emission

A significant correlation of a physical parameter with structural type is found in studies of the hydrogen emission at 21 cm. The fractional hydrogen content and the ratio of hydrogen mass to luminosity both increase in a systematic manner for later structural types

The author is a member of the staff of the National Radio Astronomy Observatory, Charlottesville, Virginia 22901.

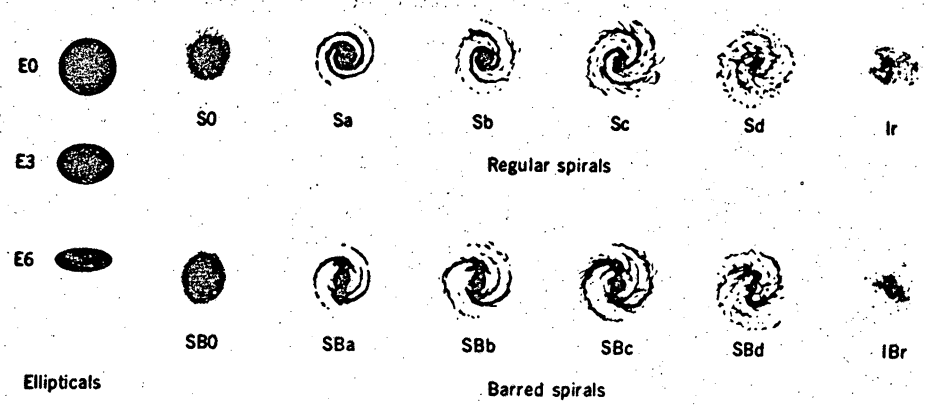

Fig. 1. Schematic representation of normal galaxy types. This is a composite of classification systems proposed by Hubble (*3*, *6*) and de Vaucouleurs (*4*).

(*8*). The significance of this correlation is not understood. When first found it was thought to be the Rosetta stone which would aid in deciphering the Hubble sequence; perhaps the clue to an evolutionary sequence was at hand. As will be discussed below, these hopes have yet to be realized. But the correlation of hydrogen content and galaxy type must surely mark a significant step in our description of galaxies.

Part of the importance of hydrogen is that it is the most abundant, by far, of all the elements; it is nine times more abundant in number of atoms and twice as abundant in mass compared to second place helium. Together, these two elements make up 99 percent of the chemical mass of the universe. Within our own galaxy most of this mass is in the form of stars. Interstellar material, dust and gas, represents about a twentieth of the total mass of the galaxy. It is, however, an important component for it is the stuff from which new stars are made.

Interstellar hydrogen occurs in both atomic and molecular states and at various levels of excitation. The first discovered radio spectral line and the only one known for 12 years arises from a hyperfine transition of neutral, atomic hydrogen (HI). The wavelength corresponding to this transition is 21 cm. It was predicted by van de Hulst (*9*) in 1944 and detected from galactic hydrogen radiation in 1951. The first extragalactic detection of 21-cm line radiation was made 2 years later. The source was the Magellanic Clouds, the two galaxies nearest the Milky Way (*10*).

This year, the 20th anniversary of such extragalactic observations, is a convenient mark for the beginning of a new era—one of high angular resolution studies of extragalactic hydrogen through beam synthesis. The first Magellanic Cloud observations were made with an antenna 36 feet (11 meters) in diameter, with a beam width at 21 cm of 1.5 degrees. The two largest filled-aperture telescopes currently used for extragalactic line studies have beam widths of 10 by 10 and 4 by ≥ 24 arc minutes. The first is obtained with the 300-foot (91 m) telescope at the National Radio Astronomy Observatory in Green Bank, West Virginia. The other is for the tiltable plane-standing parabola antenna of the Paris Observatory located in Nancay, France. The north-south beam of this instrument is dependent on declination: at approximately 30° or less the beam width is 24′, at more than 60° it becomes larger than half a degree.

The beam areas of these telescopes

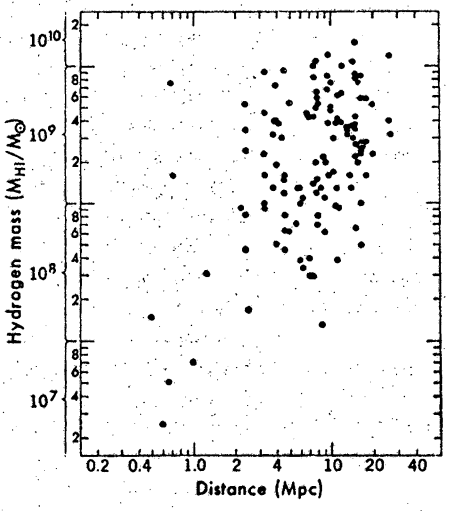

Fig. 2. Interstellar atomic hydrogen content for spiral galaxies plotted against the distance of the system. Note the rather abrupt upper limit which applies regardless of structural type.

are about 10^{-2} times that of the 36-foot telescope. Beam synthesis will give an additional improvement of about 10^{-3}. The procedure involves using an interferometer (or groups of interferometer pairs) at several spacings. These, combined with the earth's rotation, give the equivalent of an antenna beam corresponding to the separation of the interferometer elements. For 21-cm line work, spacings are generally in the range of a few hundred meters to over a kilometer. In this manner resolutions of about 2′ to 4′ have been achieved at the California Institute of Technology, Pasadena, and at Cambridge, England. The array of telescopes at Westerbork in the Netherlands is synthesizing a beam of 25 arc seconds at 21 cm.

A large body of information may be derived from studies of the 21-cm hydrogen line radiation from galaxies. This includes

1) The total hydrogen content.
2) The distribution of hydrogen.
3) The systemic radial velocity; that is, the red shift of the galaxy.
4) The radial velocity field; that is, a map of loci of constant radial velocity as seen on the projected image of the galaxy.
5) An estimate of the total mass of the system from (i) its global velocity profile or (ii) its rotation curve.

Assuming that 21-cm line radiation is detected, then the determinations of 1, 3, and 5(i) are essentially independent of the antenna beam size. The ability to determine the other parameters, 2, 4, and 5(ii), is directly related to the ratio of galaxy size (or, more specifically, hydrogen extent) to beam size. We would like this ratio, the relative resolution, to be as large as possible. The new era of high angular resolution (small beam size) will greatly increase and improve on the rather small sample of galaxies for which good relative resolution is presently available.

The past 20 years have given us extensive data on those parameters derivable from the lower resolution studies. It is primarily this material which will be reviewed here.

Hydrogen Content

Two assumptions are generally made in relating the observed brightness temperature, T_B, to the column density (projected surface density) of neutral

hydrogen: (i) that the hydrogen is optically thin, and (ii) that there is no interaction with any continuum radiation. Under these conditions the column density $N(\theta,\phi)$, in atoms per square centimeter, at position θ,ϕ is given by

$$N(\theta,\phi) = 1.823 \times 10^{18} \times \int_{-\infty}^{+\infty} T_B(\theta,\phi,V_r)dV_r \quad (1)$$

where the integration is over all radial velocities (V_r) expressed in kilometers per second. Typical beam-averaged values of N lie in the range 10^{20} to 10^{21} atoms per square centimeter.

The total hydrogen mass in solar units, $M_{HI}/M_\odot$, is obtained by integrating over the galaxy

$$M_{HI}/M_\odot = 1.236 \times 10^{3} D^2 \times \iiint T_B(\theta,\phi,V_r)\, d\theta\, d\phi\, dV_r \quad (2)$$

where D is the distance to the galaxy in megaparsecs and the coordinates are expressed in arc minutes. The integration is over all radial velocities (kilometers per second) and the convolution of the main beam and the source, for example, the observed contour diagram. Hydrogen masses are typically 10^9 $M_\odot$.

A convenient form of Eq. 2, especially for estimating an upper limit, is

$$M_{HI}/M_\odot = 1.5 \times 10^{8} D^2 T V \theta_1 \theta_2 \quad (3)$$

where T is the peak brightness temperature, V is the half-intensity width of an assumed Gaussian velocity distribution, and θ_1 and θ_2 are the half-intensity widths of the beam-averaged HI spatial distribution (taken here as Gaussian in shape). For an upper limit θ_1 and θ_2 refer to the beam size.

The neutral hydrogen content for 130 spiral and irregular galaxies is shown in Fig. 2, where the derived hydrogen mass is displayed as a function of distance. (The distances are from a variety of sources; many are from systemic velocities and a Hubble constant (H) of 100 km sec^{-1} Mpc^{-1}.) The diagonal boundary in the lower right of this figure reflects the observational constraint of the inverse square law. Of more interest is the strikingly sharp boundary along the top of the figure. To within less than a factor of 2, the upper boundary to the neutral hydrogen content of a galaxy is 10^{10} $M_\odot$. The upper boundary cannot be explained as a selection effect, for observational selection generally favors galaxies having a high hydrogen content. Rather it reflects a real boundary. Galaxies appear to have a self-regulating mechanism; given more than 10^{10} $M_\odot$ of hydrogen they will convert it to some other form. Possibilities include molecular hydrogen, regions of high optical depth, or stars. If galaxies with more than 10^{10} $M_\odot$ of hydrogen exist, they have not yet been recognized.

Three sources of error or uncertainty are present in hydrogen mass determinations. (i) Observational errors include poor signal-to-noise ratio, incomplete mapping of the source, calibration uncertainties, and so forth. When the results of various observers are intercompared and zero-point differences are corrected, the typical scatter is 20 to 30 percent, although much larger individual differences are found. (ii) The distance to the galaxy is uncertain (see Eq. 2). This is an all too common problem in astronomy, especially in extragalactic studies. For this reason parameters which are independent of distance are of particular interest. These include hydrogen surface density and

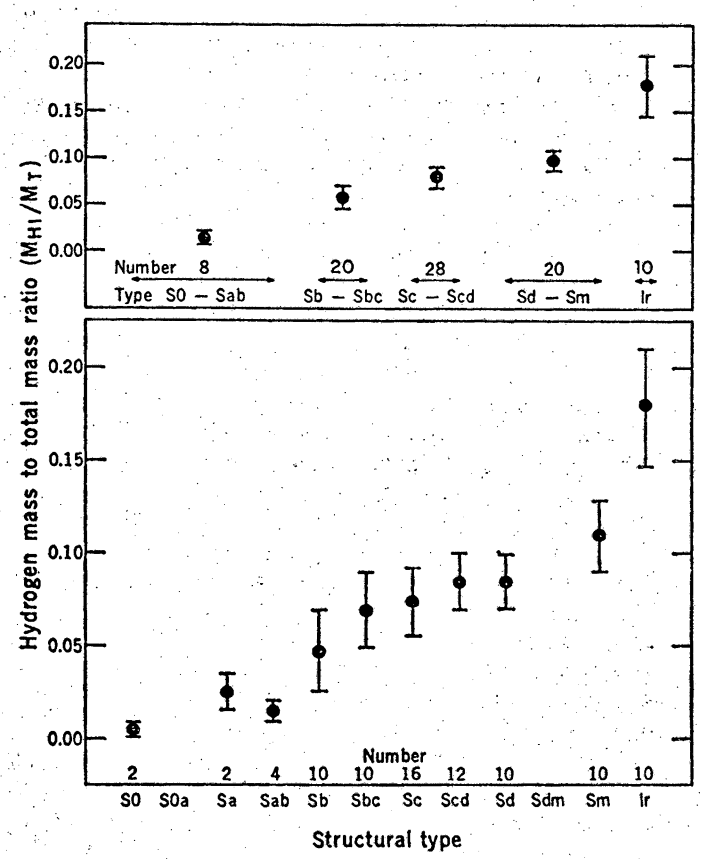

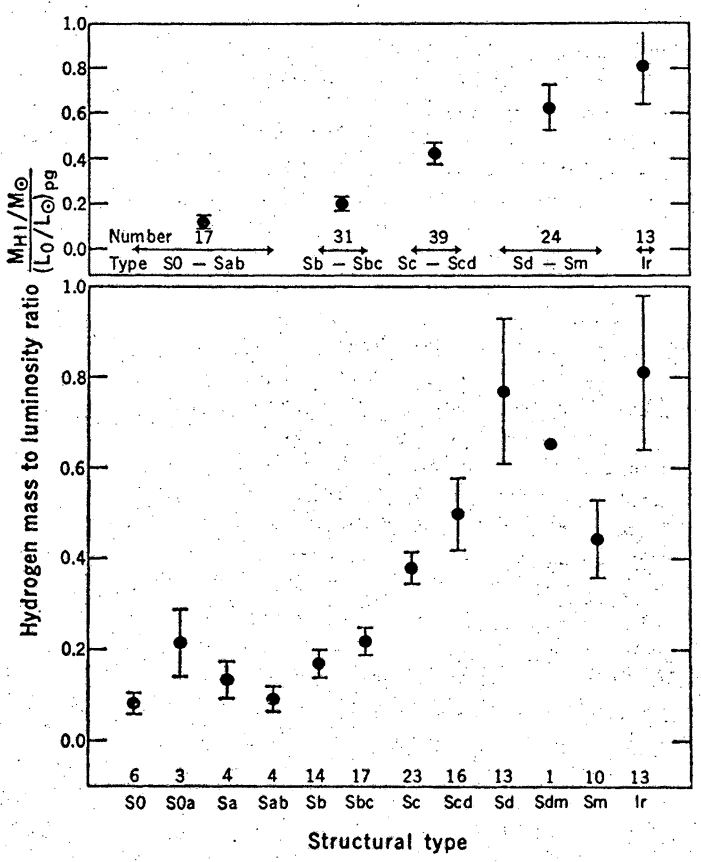

Fig. 3 (left). Fractional hydrogen content for galaxies of different structural type. The upper panel represents averages over several structural classes. Fig. 4 (right). Ratio of hydrogen mass to photographic (pg) or blue luminosity for galaxies of different structural type. The upper panel represents averages over several structural classes.

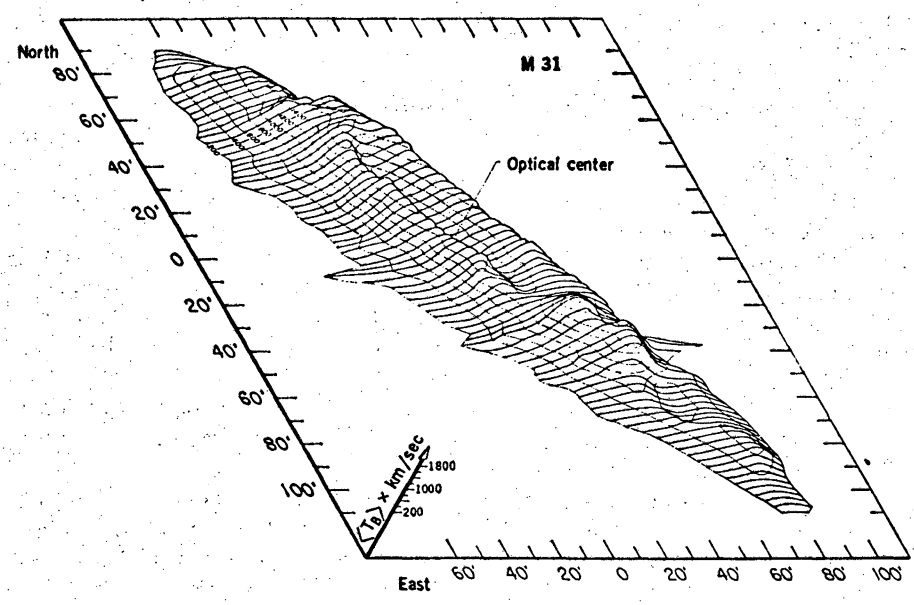

Fig. 5. Isometric projection of the integrated brightness temperature contours for M 31, the Andromeda Nebula; the units are °K × kilometers per second. These contours are directionly proportional to the projected surface density of hydrogen with 1000°K km $sec^{-1} = 1.8 \times 10^{21}$ atoms per square centimeter. The beam size is 10'.

the ratio of hydrogen mass to optical luminosity. (iii) The validity of the assumption of small optical depth is uncertain. This assumption appears to hold in general for our galaxy, although there are many regions of high optical depth. Because of the assumption of small optical depth, the hydrogen content of a galaxy is underestimated. The exact amount is not known but is most likely less than a factor of 2. This uncertainty may be described as intrinsic to the system and reflects local regions of high density. Another optical depth effect enters through the inclination, *i*, of the galaxy. The line of sight will be longer through an edge-on system than through a face-on one. Countering this is the greater radial velocity range in the former case. By using suitably normalized hydrogen masses for a large number of galaxies, an inclination effect has been found. Galaxies with *i* greater than 60° have a lower observed HI mass. This may be allowed for through a statistically derived correction (*11*).

The fractional hydrogen mass content of a galaxy, M_{HI}/M_T (T = total), varies with structural type. It is about 1 percent in the earliest type spirals, S0, and reaches 18 percent for the latest type spirals, the irregular systems. This variation is displayed in Fig. 3. The systematic variation of this ratio with type is one of the few correlations of a quantitative parameter with structural type.

No elliptical type galaxies are included in Figs. 2 and 3. Only one positive detection has been reported (*12*) and this has been questioned by more recent observations which set upper limits of several times $10^8 M_\odot$ for the mass of optically thin neutral hydrogen (*13*). This gives typical values of M_{HI}/M_T of less than 10^{-3}. This very low upper limit is puzzling, for we believe that stars, as they evolve, return material to the interstellar matter and that detectable amounts (that is, well above the observed limits) should soon accumulate. There have been several suggestions to explain this discrepancy (*13*). These include sweeping out of the gas by an intergalactic wind, or collection of the material in the central region of the elliptical galaxy with a resultant triggering of the formation of either a star or a very massive object.

The helium content of the interstellar medium for different regions within a galaxy, as well as for different types of galaxies, appears to be remarkably constant (*14*). The number ratio of helium to hydrogen atoms is 0.11. Thus, the fraction of the total mass in the form of interstellar gas (HI and He) for the average irregular type galaxy is one-fourth. In our own galaxy it is about one-twentieth.

The hydrogen content of a galaxy may also be compared to its optical luminosity, L_o. A convenient and common measure of the latter is the magnitude in the photographic or blue part of the spectrum, appropriately corrected for inclination and foreground galactic extinction. The ratio M_{HI}/L_o in solar units is shown in Fig. 4 as a function of structural type. It is independent of distance since both the hydrogen radiation and the luminosity radiation depend in the same manner on distance. The steady increase in this ratio with later type systems is evident in the upper panel of Fig. 4. In the lower panel the apparent drop for type Sm may reflect uncertainty in the optical depth–inclination correction mentioned above. This correction is most likely dependent on galaxy type, but there are too few data at present to make such a subdivision. Most of the sample of ten Sm's are of high inclination and the correction may have been underestimated for this structural class.

The ratio of hydrogen mass to luminosity is another physical parameter that is well correlated with structural type. This ratio also implies a characteristic time scale for galaxies in which they may maintain their present luminosity L_o by converting their hydrogen into stars (*7*). After applying various corrections to allow for mass returned to the interstellar medium and to obtain the bolometric magnitude of the young stars within a galaxy (rather than the total photographic magnitude), one finds that all types of spirals may maintain their present rate of star formation for a few times 10^{10} years. This argument may be inverted to show that an approximate doubling of the interstellar mass will allow galaxies to have maintained their present rate of star formation for about a Hubble time ($1/H$). Thus, the large amounts of gas in late type systems (and more specifically the sample of late type systems represented by the data in Figs. 2, 3, and 4) need not imply that they are young. All spirals studied in this manner may be of the same age. The variation in hydrogen content may only reflect the efficiency of converting interstellar gas into stars, the irregulars being least efficient and the early type spirals most efficient.

Hydrogen Distribution

Two criteria describe the ability to map details in another galaxy: (i) the relative resolution given by the ratio of source size to beam size, which we want as large as possible, and (ii) the linear scale of the beam at the distance

of the source. As examples consider the Andromeda galaxy at a distance of 0.69 Mpc and a member of the Virgo cluster of galaxies at 12 Mpc. In Virgo, the larger spiral systems are about 10′ in diameter. For the 10′ beam of the 300-foot telescope the relative resolutions are about 30 and 1, respectively. The linear scale is 10′ equals 2 kpc and 24 kpc for the two examples. These linear scales refer to distances measured on the plane of the sky; any nonzero inclination will have a foreshortening for positions off the major axis, the line defined by the intersection of the plane of the galaxy and the plane of the sky.

For Andromeda there is a good coincidence between the optical features which define the spiral arms and the regions of high surface density of hydrogen (*15*). This coincidence is most meaningful along the major axis where the linear resolution in the plane of the galaxy is highest. Coincidence with 10′ beam radio observations are also found off the major axis, but the foreshortening ratio of more than a factor of 4 makes such comparison less meaningful. Observations with higher resolution are required.

The highest linear resolution with a filled aperture was obtained with the combination of the 210-foot (64-m) antenna at Parkes, Australia, and the Magellanic Clouds—the linear resolution is 0.25 kpc. At first sight both clouds are irregular in nature, clearly defined optical spiral features are not present. A more careful study of the Large Cloud shows that its luminous features define a "one-armed" spiral and it is a prototype of the Sm category of spiral (*16*). Good coincidence in both position and velocity is found between the extensive small-scale clumps of neutral hydrogen and ionized hydrogen (HII) (*17*).

The following picture is emerging from the results obtained with both filled-aperture and aperture synthesis telescopes. All galaxies showing spiral structure, including our own, show a minimum in the projected surface density of hydrogen in the center of the galaxy. This is evident in the integrated brightness temperature map for M 31 shown in Fig. 5. Synthesis results for the galaxy M 33 (*18*) which are in conflict with this conclusion appear to be in error (*19, 20*). The surface density reaches a maximum at some distance from the center. For Andromeda this maximum occurs at about 10 kpc, for our galaxy at about 12 kpc. The hydrogen distribution decreases from this maximum value with increasing distance from the center. A gross oversimplification of the distribution is to describe it as a "ring."

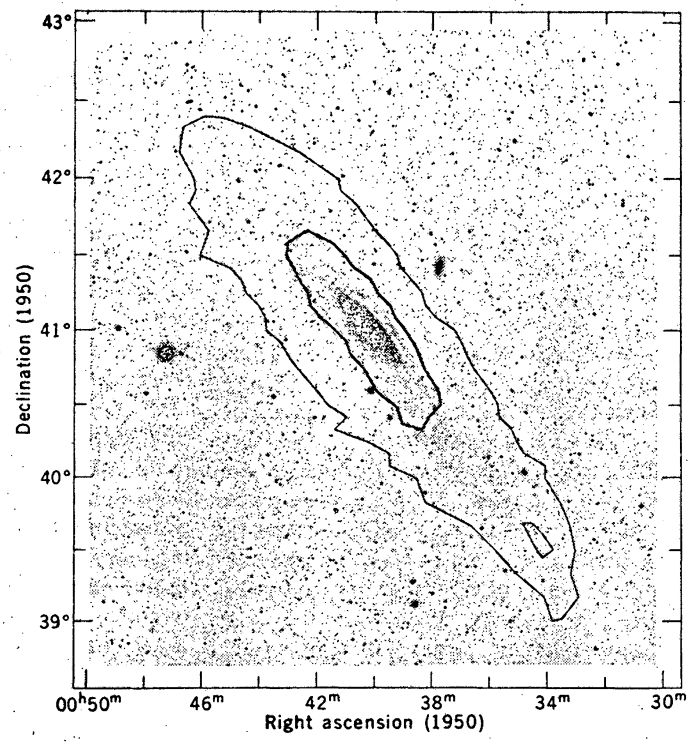

Fig. 6. Two contour levels of integrated brightness temperature superimposed on a photograph of M 31. The inner, heavier contour is for peak values. The outer, lighter contour is 200°K km sec^{-1} and is one-sixth to one-eighth the peak values. A hydrogen concentration in the southwest is outlined by a contour of 600°K km sec^{-1}. The beam size is 10′. The year 1950 is the epoch or date to which the coordinates are referred.

For the early type galaxies, the spiral arms are embedded in this ring—in the region of highest HI surface density. For later type galaxies significant parts of the prominent spiral arms are found interior to the region of maximum HI surface density. Much confusion has originated over this point because parts of spiral arms and, at times, whole arms—but of low surface brightness—are found in the region of maximum hydrogen density. There is as much correlation as anticorrelation between many of the bright optical and HI concentrations in late type spirals. What is of importance here is that so much of the prominent arms is not located in regions of greatest hydrogen distribution. In the latest type systems—the irregulars—the central minimum is gone, replaced by a central maximum with the prominent optical features distributed throughout this maximum.

The depth of the central minimum varies, possibly with total mass of the galaxy. It is the small contrast between the central minimum and the maximum HI region in M 33 that has resulted in the conflicting results mentioned above.

No satisfactory explanation for this HI distribution is available although several have been suggested (*21*). The data are few (only ten galaxies) and a subdivision by type makes each category woefully small. Additional information can only come from synthesis telescope observations.

The decrease in hydrogen column density (and hence brightness temperature) at large distances from the center of a galaxy places a severe signal-to-noise limitation on the determination of the extent of hydrogen. This is especially so for synthesis observations unless unusually long integration times are employed. Filled-aperture observations are more favorable, but the beam size limitation restricts such studies to galaxies of large angular size. Because the signals are weak, special attention must be directed to the beam shape and to beam side-lobes.

The 300-foot telescope has been used to study all of the larger galaxies and they all show hydrogen dimensions significantly larger than optical dimensions measured to a sky-limited surface brightness. Such an effect was first described by Dieter (*22*). At a radial distance of 28 kpc, Andromeda has a column density of about 10^{20} atoms per square centimeter (see Fig. 6). The galaxy M 81 is surrounded by a hydrogen "envelope" which includes its companion galaxies M 82 and NGC 3077 (*14*). At 30 kpc the hydrogen column density is also about 10^{20} atoms per square centimeter. Generally this greatest extent in hydrogen is found near

but not on the major axis. A prominent example is M 33 where Gordon (*20*) has mapped two "wings" of hydrogen at about 40° from the major axis. His results have been extended with later measurements and the northern wing has been mapped to 75′, or approximately 15 kpc; the optically measured radius is about one-half this value. The hydrogen along the major axis has an extent of about 50′ or 10 kpc.

If the mean surface density of hydrogen is determined by using optically derived dimensions a strong correlation with type is found, in the sense that later type galaxies have higher surface densities (*11*). In an extensive study of moderate-sized galaxies (in angular extent) Bottinelli (*23*) concluded that the ratio of hydrogen size to optical size varies with type, with the later galaxies having larger ratios (*23*). The surface density–type correlation is no longer present when hydrogen rather than optical dimensions are employed. Bottinelli's conclusions are important and warrant independent confirmation.

Red Shifts

The red shift, or the systemic radial velocity, as measured by observations of the 21-cm emission, is available for well over 100 systems. The major fraction of these come from Green Bank and Nancay and there is excellent agreement between values for galaxies in common. Comparisons between 21-cm and optical determinations give a powerful test of the form of the Doppler expression over a wavelength ratio of half a million. It is important to note that optical and radio astronomers use different conventions for computing the velocities (V). In the optical case, wavelengths are measured and the quantity $c\Delta\lambda/\lambda_0 = V_{opt}$ is employed (c is the velocity of light, λ the observed wavelength, and λ_0 the wavelength at rest). In radio astronomy frequencies (ν) are the measured quantity and velocities are given as $c\Delta\nu/\nu_0 = V_{radio}$. These are not equal, rather

$$c\Delta\lambda/\lambda_0 = c\Delta\nu/\nu \qquad (5)$$

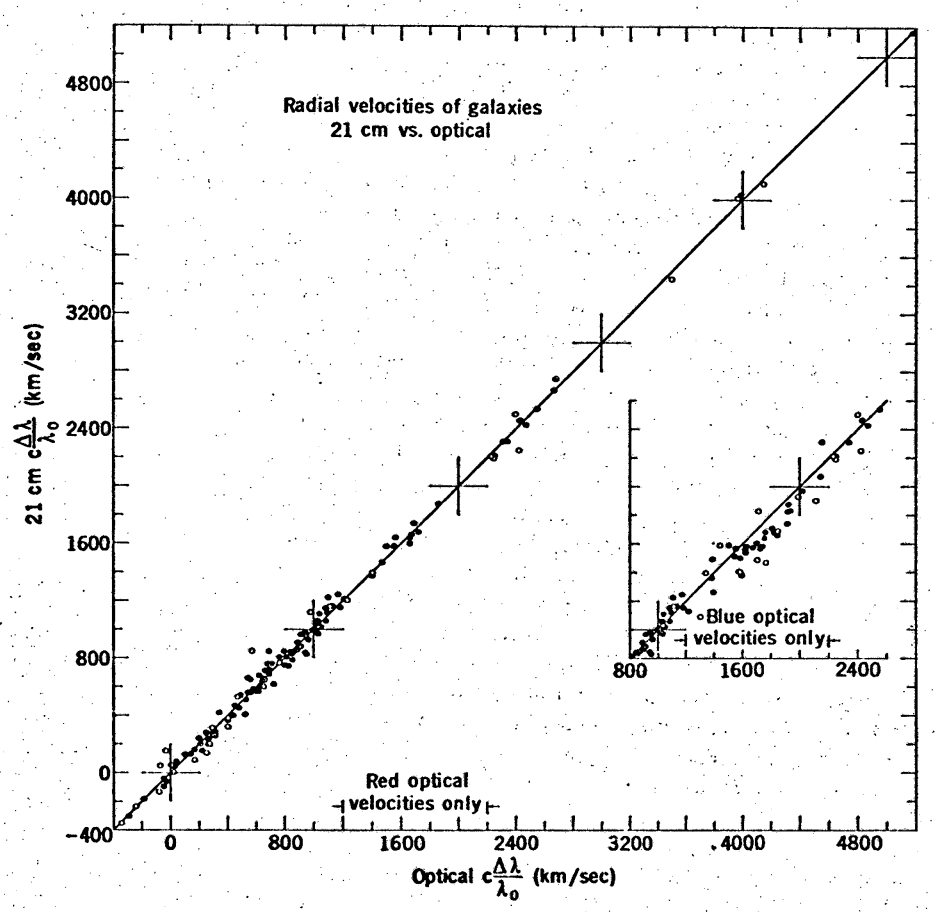

Fig. 7. Comparison of red shifts of galaxies measured at 21 cm and at optical wavelengths. The inset shows the region of discrepancy (1200 to 2200 km sec^{-1}) which occurs with optical measurements made in the blue part of the spectrum. Only values derived from the red part of the spectrum are used in this velocity range in the main body of the diagram. Filled circles are points of normal weight and open circles points of low weight. The large plus signs are added for convenience in reading the coordinates.

For small velocities, less than 1000 km sec^{-1}, the difference is 3 km sec^{-1}, but at 5000 km sec^{-1} the difference reaches 85 km sec^{-1}. The importance is that it represents a systematic effect and must be allowed for in comparing optical and 21-cm determinations. Such a comparison is made for 136 galaxies in Fig. 7, where both axes are expressed in the optical convention.

Over the range of about −400 to 5200 km sec^{-1} there is excellent agreement. The two regression solutions for these data agree to within the thickness of the line drawn in Fig. 7. However, there is a systematic difference of about 100 km sec^{-1} in the range of about 1200 to 2200 km sec^{-1}, as shown by the inset in Fig. 7. An analysis of the various optical data shows that this effect is present only when the optical measurement was made from blue-sensitive spectra. Red spectra, where the Hα line of hydrogen and the forbidden [NII] line of nitrogen are generally measured, do not show the systematic difference. The cause has not been definitely established, but it is most likely contamination of the galaxian Fraunhofer H and K lines by similar absorption lines in the night sky. In the main body of Fig. 7 only optical values measured in the red have been used in the range of disagreement. The rest of the data are based on any optical measurements available (*14*).

Velocities greater than those indicated in Fig. 7 have recently been measured at 21 cm. Hydrogen has been observed in emission at 6600 km sec^{-1} and in absorption at 8120 km sec^{-1}. In both cases (galaxies NGC 7319 and NGC 1275, respectively) there is good agreement with optically measured values (*24*).

We may conclude that the form of the Doppler expression holds over a wavelength range of 5×10^5 and over an equivalent velocity range of −400 to 8000 km sec^{-1}. Such measurements serve as a test of the constancy, with time, of the ratio of magnetic moments of the proton and the electron (*25*). The equality of the 21-cm and optical velocities indicate, within large errors, a constancy in this ratio over the range of velocities available.

A significantly larger 21-cm red shift has been measured in absorption in the spectrum of the quasar 3C 286 (*26*). The line is shifted from 1420.4 to 839.4 megahertz, corresponding to $z_{21,abs} = \Delta\lambda/\lambda_0 = 0.692$. The velocity profile is shown in Fig. 8. The red shift of the optical emission line is $z_{em} = 0.849$.

This difference between z_{abs} and z_{em} follows the usual pattern for optical measurements where, nearly always, $z_{abs} \lesssim z_{em}$. The 21-cm line is quite narrow, corresponding to a half-width of 8.2 km sec^{-1} in the rest frame. Such a narrow line is difficult to measure optically in a faint object (the visual magnitude of 3C 286 is 17.25). However, if optical absorption lines are eventually detected in 3C 286 and have red shifts corresponding to $z_{21,abs}$ then a stringent test on the above constancy comparisons becomes available. Such optical absorption lines together with the 21-cm line will also yield information on the ionization state of the absorbing gas.

Because of the narrowness of the line and the difference between z_{em} and $z_{21,abs}$ it seems likely that an intervening galaxy along the line of sight to 3C 286 is responsible for the absorption line (*26*).

Radial Velocities and Dynamics

The Doppler shift of the 21-cm line reflects the systemic motion of a galaxy as a whole as well as the radial component of motions of the hydrogen within the system. For galaxies significantly larger than the telescope beam such data can be used to construct a radial velocity map of the galaxy. Comparison with computer-generated models yields such galaxian parameters as the inclination of the plane, the position angle of the major axis, the rotation curve, and the systemic velocity. Observationally, the data are influenced by the beam size, hydrogen distribution, and velocity field, and the model must include all of these parameters for a realistic comparison with the observed data. This approach has been employed in varying degrees of complexity at Green Bank, Nancay, and Pasadena.

Most of the galaxies studied so far are comparable in size to the beam width, and radial velocity maps cannot be derived. Instead the basic observable parameter is the global velocity profile, a display of signal strength versus radial velocity. The area under this curve yields the hydrogen content of the galaxy (see Eq. 2). The midpoint of the profile is a measure of the systemic radial velocity. The width of the profile may be used to derive an estimate of the total mass of the galaxy. This width is primarily determined by the ordered motion within the galaxy, that is, rotational and possible radial

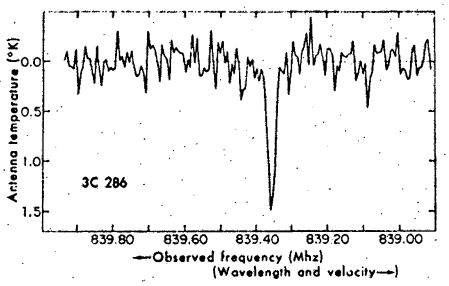

Fig. 8. Absorption profile in the direction of the quasi-stellar object 3C 286. The 21-cm hydrogen line has been shifted from 1420 to 840 Mhz, corresponding to $z = 0.692$.

streaming. The profile would have sharp, vertical edges for the case of no random motions and infinitely narrow filters. Random motions and finite filter widths act to broaden and taper the edges of the profile. For a pure rotational model, the half-width of the profile (after correction for random motion and filter width) measures the peak of the rotation curve. This parameter, together with a statistically derived value of the location of the peak, in terms of the optical dimensions of the galaxy, yields a good estimate of the total mass of a highly concentrated mass model (*11*).

A distributed mass model may be accounted for by an additional parameter, n, which is related to the shape of the rotation curve (which, in turn, reflects the mass distribution). At present, the same value of n is used for all spiral galaxies, regardless of structural type. A systematic error as a function of structural type will occur if n varies with type. There is a suggestion that this may be the case, as shown below. A comparison between galaxies whose masses have been determined by both

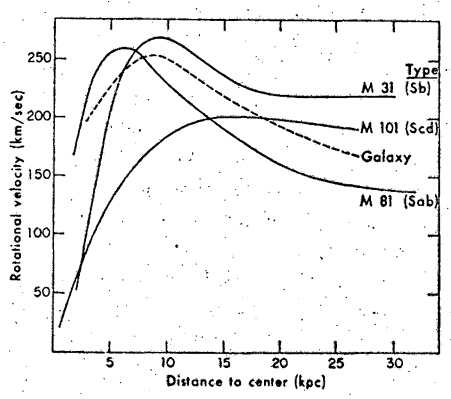

Fig. 9. Observed rotation curves for three spiral galaxies of different structural type. The rotation curve for our galaxy is shown as a dashed line. At distances greater than 10 kpc the galactic curve is based on an assumed mass distribution.

21-cm and optical methods shows no dependence on type. In the mean, the radio determinations yield a total mass estimate which is twice that of the optical determinations (*11*). This is a surprisingly good agreement considering the uncertainty in both types of determinations. Further, it is not clear which approach is responsible for the "error." Most of the optical determinations are lower limits because they refer to the mass within the last measured point. In comparing masses determined by both methods an attempt is made to correct for this underestimation, but little is known of the form of the rotation curve at large distances from the center.

This problem has been tackled by 21-cm techniques, where observations at such large distances are more feasible than they are for optical measurements. Three rotation curves extending to large distances have been derived so far, and the available data from optical, aperture synthesis, and single dish measurements are combined and displayed in Fig. 9 (*27*). The sample, although small, is a fortunate one, for three different types or subtypes are represented: Sab, Sb, and Scd. Although the total masses of these systems are similar (approximately 10^{11} $M_\odot$) their rotation curves and hence the mass distribution within the systems differ quite significantly. The determination of specific values of the mass distribution depends on the model used since only three of the six necessary phase space quantities are available from observation. But it is simple to show (and model calculations confirm) that the mass distribution varies with structural type for these three galaxies. The earliest type is more centrally condensed. This conclusion has generally been assumed to hold—on the basis of the distribution of luminosity within the different types of galaxies—but it has never, to my knowledge, been demonstrated.

Another aspect of the rotation curves in Fig. 9 is their great extent, well beyond the usually adopted optical boundaries (see Fig. 6). There must be significant mass at these great distances. It is not in the form of neutral hydrogen. Thus, at 28 kpc in Andromeda (M 31) only about 3 percent of the projected surface density is in the form of hydrogen. Stars of the most common type, M dwarfs, could account for the necessary mass. The total luminosity of these stars would be about 1 percent of the sky brightness in the blue and would thus remain undetected in usual photomet-

ric studies. If the mass is indeed in late type dwarfs, observations in the far-red or infrared should uncover them.

Keeping in mind the various uncertainties and assumptions involved in deriving the total mass of a galaxy, we will proceed to examine the available data. Figure 10 shows "total" masses for different types of spiral galaxies. They have been derived from optical and from 21-cm studies.

As a statistical sample they must be considered with extreme caution for serious selection effects are present which favor intrinsically massive systems. This sample is not representative of galaxies per unit volume of space. Several conclusions may be drawn from Fig. 10: (i) Among the most massive spirals, the late type systems (Sm and Ir) are, on the average, less massive than earlier type ones. (ii) There is no clear-cut difference in either the mean or the maximum mass for types S0 to Sd. This conclusion is affected by the uncertainty in individual mass determinations and by the small sample size for the very earliest types. (iii) Intermediate and early type spirals with masses less than 10^{10} $M_\odot$ are either exceedingly rare or this group has been seriously undersampled. (iv) There appears to be an upper bound of about 10^{12} $M_\odot$ to the total mass of a spiral.

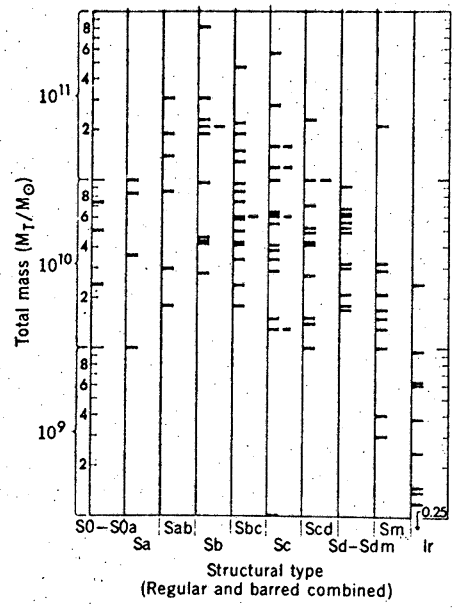

Fig. 10. Total masses of spiral galaxies of different structural types. The data are from both optical and 21-cm determinations.

Except for the very latest systems, the total mass of a spiral does not appear to be correlated with type.

Red shifts of galaxies measured at optical wavelengths and at 21 cm are in excellent agreement. The form of the Doppler expression has been shown to hold over a wavelength range of 5×10^5.

All spirals earlier than type Ir which have been studied with adequate resolution show a central minimum in their hydrogen distribution. The region of maximum projected HI surface density occurs at some distance from the center. In the earlier type spirals the optical arms are located in the region of this maximum surface density. In the later type spirals the maximum HI density and prominent optical arms are less well correlated and, at times, are anticorrelated.

Detailed studies of the HI distribution and motions within a galaxy require the high relative resolution of beam synthesis arrays. We may expect significant new information from such studies, which are now in progress. Filled-aperture telescopes will supply the necessary observations at zero spacing and vital statistical information on large numbers of galaxies, peculiar systems and groups and clusters of galaxies. The two types of telescope systems will complement one another. In the near future we should have a much better description of spiral galaxies and, we hope, a better understanding of these systems.

Summary

Measurement of the 21-cm line radiation originating from the interstellar neutral hydrogen in a galaxy yields information on the total mass and total hydrogen content of the galaxy. The ratio of these two quantities is correlated with structural type in the sense that the later type galaxies contain a higher fraction of their total mass in the form of interstellar hydrogen. This ratio is one of the few physical parameters known to correlate with structural type. It need not, however, reflect an evolutionary sequence, such as more hydrogen implying a younger galaxy. Efficiency of conversion of hydrogen to stars can just as easily explain the correlation.

References and Notes

1. E. Hubble, paper read at the 33rd meeting of the American Astronomical Society, held in affiliation with the American Association for the Advancement of Science, 30 December 1924 to 1 January 1925, Washington, D.C.; abstracted in *Pop. Astron.* **33**, 252 (1925).
2. E. Oepik (now spelled Opik), *Astrophys. J.* **55**, 406 (1922).
3. A. Sandage, *The Hubble Atlas of Galaxies* (Publ. No. 618, Carnegie Institution of Washington, Washington, D.C., 1961).
4. G. de Vaucouleurs, in *Hanbuch der Physik*, S. Flügge, Ed. (Springer-Verlag, Berlin, 1959), p. 275.
5. H. Arp, *Atlas of Peculiar Galaxies* (California Institution of Technology, Pasadena, 1966).
6. E. Hubble, *The Realm of the Nebulae* (Dover, New York, 1958), p. 38.
7. M. S. Roberts, *Annu. Rev. Astron. Astrophys.* **1**, 149 (1963).
8. ———, in *Stars and Stellar Systems: Galaxies and the Universe*, G. P. Kuiper and B. M. Middlehurst, Eds. (Univ. of Chicago Press, Chicago, in press), vol. 9.
9. H. C. van de Hulst, *Ned. Tijdschr. Natuurk.* **11**, 201 (1945).
10. F. J. Kerr and J. V. Hindman, *Astron. J.* **58**, 218 (1953); F. J. Kerr, J. V. Hindman, B. J. Robinson, *Aust. J. Phys.* **7**, 297 (1954).
11. M. S. Roberts, *Astron. J.* **74**, 859 (1969).
12. B. J. Robinson and J. A. Koehler, *Nature (Lond.)* **208**, 993 (1965).
13. J. S. Gallagher III, *Astron. J.* **77**, 568 (1972).
14. M. S. Roberts, in *External Galaxies and Quasi-Stellar Objects, IAU Symposium No. 44*, D. S. Evans, Ed. (Reidel, Dordrecht, Netherlands, 1972), p. 12.
15. ———, *Astrophys. J.* **144**, 639 (1966); in *Radio Astronomy and the Galactic System, IAU Symposium No. 31*, H. van Woerden, Ed. (Academic Press, London, 1967), p. 89.
16. G. de Vaucouleurs, *Astrophys. J.* **131**, 265 (1960).
17. R. X. McGee, *Aust. J. Phys.* **17**, 515 (1964); ——— and J. A. Milton, *ibid.* **19**, 343 (1966).
18. M. C. H. Wright, P. J. Warner, J. E. Baldwin, *Mon. Not. R. Astron. Soc.* **155**, 337 (1972).
19. D. Rogstad, I. Lockhart, M. Wright, unpublished results of observations with the interferometer at the California Institute of Technology, communicated by D. Rogstad.
20. K. J. Gordon, *Astrophys. J.* **169**, 235 (1971).
21. G. S. Shostak, thesis, California Institute of Tehnology (1972).
22. N. H. Dieter, thesis, Harvard University (1958); *Astron. J.* **67**, 317 (1962).
23. L. Bottinelli, *Astron. Astrophys.* **10**, 437 (1971).
24. For NGC 7319: C. Balkowski, L. Bottinelli, P. Chamaraux, L. Gouguenheim, J. Heidmann, *ibid.*, in press; G. Shostak, *Astrophys. J.*, in press. For NGC 1275: D. S. DeYoung, M. S. Roberts, W. C. Saslaw, *ibid.*, in press.
25. A. Yahil, in *History of the Interaction Between Science and Philosophy, Sambursky Festschrift*, Y. Elkans, Ed. (Humanities, New York, 1972).
26. R. L. Brown and M. S. Roberts, *Astrophys. J.* **185**, 809 (1973).
27. M. S. Roberts and A. H. Rots, *Astron. Astrophys.* **26**, 483 (1973).
28. The National Radio Astronomy Observatory is operated by Associated Universities, Inc., under contract with the National Science Foundation.

DISTRIBUTION AND KINEMATICS OF NEUTRAL HYDROGEN IN M81

Arnold H. Rots
Kapteyn Astronomical Institute
University of Groningen, The Netherlands

Messier 81 is a large, early-type (Sab) spiral galaxy in Ursa Major. I shall assume it to be at the same distance as NGC 2403 which has been reckoned by Tammann and Sandage (1968) to be 3.25 (±0.20) Mpc distant.

This contribution reports on neutral hydrogen line observations of M81 obtained with the Westerbork Synthesis Radio Telescope as a joint project of Leiden Observatory and of the Kapteyn Institute at Groningen. The work in Leiden has been directed by Dr. W.W. Shane. The present data are in a sense still incomplete, since probably the large spatial components of the HI distribution are lacking. From the previously published observations it is not clear how much HI there really is in and around M81.

However, here I shall confine myself to those aspects which are supposed to be the least affected by this incompleteness, namely the spatial distribution of HI and its kinematics. I shall not attempt to compare the present data with previously obtained results (e.g. Roberts, 1972; Gottesman and Weliachew, 1975). For a more thorough discussion I may refer to Rots (1974).

Observations

The observations were carried out with the Westerbork Synthesis Radio Telescope employing its 80 channel filter spectrometer. The halfwidth of the filters is 27 km/s. The angular resolution is 23.9" x 25.6"; this corresponds to 380 x 400 pc at the distance of 3.25 Mpc, or 400 x 800 pc in the plane of the galaxy.

Distribution of neutral hydrogen

Fig. 1 shows the distribution of HI in the form of a "radiograph". It shows the spiral structure of the HI distribution very clearly. These spiral arms line up very well with the optical arms.

In the central regions there is a distinct deficiency of HI. In the very outer regions of the galaxy, at the eastern side two large hydrogen complexes are present; concentration I at $\alpha = 9^h54^m$, $\delta = 69^o18'$, and concentration II at $\alpha = 9^h53^m$, $\delta = 69^o33'$. These concentrations line up very well with a third concentration just south of M82, as revealed by a preliminary inspection of HI data in that area. Fig. 2 is an overlay of the hydrogen distribution over a 48-inch Schmidt photograph. Concentration I is close to, but not coincident with the irregular dwarf galaxy DDO 66/Ho IX.

In Fig. 3 the surface density distribution of neutral hydrogen as seen from a face-on position is simulated. The scale along the minor axis has been expanded such that the linear scales along the major and minor axes in the plane of the galaxy are equal. The column densities have been multiplied by cos 59^o. This figure clearly shows the symmetry of the spiral pattern which can be approximated (as indicated in the figure) by a logarithmic spiral with a pitch angle of 15^o. The spiral arms persist from 3 to 13 kpc distance from the centre of the galaxy, although they are most prominent between radii of 3 and 10 kpc. Beyond 10 kpc two outer spiral arms develop close to the line of nodes.

The spiral structure of the HI is displayed more quantitatively in Fig. 4 which shows the surface density of neutral hydrogen (= approximated column density along a perpendicular to the plane of the galaxy) averaged over spiral sectors, as a function of the azimuthal displacement of these spiral sectors in the plane of the galaxy with respect to the eastern spiral arm. The sectors extend over 2 kpc in radius and the average surface density is shown for three such ranges in radius. The peak around spiral phase = 0^{o} corresponds to the eastern arm, the peak around 180^{o} to the western arm.

Fig. 5 shows the same for the color index B-V as obtained from the observations by Brandt et al. (1972). The spiral arms show up as blue dips in this figure. There is a time lag between the regions with the bluest color and with the highest HI surface density. Assuming a pattern speed of 20 km/s/kpc this lag is of the order of 10 million years, according to the rotation curve.

Dynamics

The velocity field within a radius of 10 kpc as obtained from the HI observations is displayed in Fig. 6. The lines of equal line-of-sight velocity have been dashed in regions where the signal-to-noise ratio was poor. In the northern half apparently anomalous velocities occur in the region of the northern outer arm.

From this velocity field I derived values for the position angle of the receding half of the major axis ($332^{o}\pm3$), for the inclination angle between the plane of the galaxy and the plane of the sky ($59^{o}\pm2$), and for the (heliocentric) systemic velocity (-40 km/s$\pm$5).

The resulting rotation curve is shown in Fig. 7. Within 3 kpc there is not enough HI to determine the curve reliably. Between 3 kpc and 10 kpc there is general agreement between the northern and southern halves of the galaxy. Outside 10 kpc the two halves deviate from each other. This discrepancy is connected with the anomalous velocities in the northern outer arm region and might be caused by tidal effects due to M82. One would then also expect non-circular motions in the corresponding region in the southern half. At present, however, it is not yet possible to clarify the influence of tidal effects; this requires a study of M81 and all its companions which will be done in the near future.

For fitting a mass model I decided to extend the rotation curve beyond 10 kpc with points from the southern half, rather than from the northern half or the mean of the two halves, because it produces the simplest mass model. The model I fitted is of the type described by Shu et al. (1971), consisting of flattened inhomogeneous spheroids and a thin disk component. The rotation curve produced by this model is also shown in Fig. 7.

Fig. 8 shows the mass surface density from this model, together with the blue and yellow surface luminosities. These luminosities were derived from the observations by Brandt et al. (1972), corrected for galactic and internal extinction, and averaged in circular rings, 250 pc wide in the plane of the galaxy. The mass-to-luminosity ratio remains between 2.5 and 6, except perhaps for the central regions where the mass model and the internal absorption are much less well known.

Linear density-wave theory

I attempted to fit a model velocity field based on linear density-wave theory, as described by Lin et al. (1969), and according to the formulae given by Burton (1971) and Rogstad (1971), to the residual velocity field. This residual field was obtained by subtracting the circular motions according to the mass model from the observed line-of-sight velocities.

For this fit I used the rotation curve and the epiclyctic frequencies as derived from the mass model. Because the HI spiral arms are unperturbed between 3 and 10 kpc, I assumed a pattern speed of 20 km/s/kpc which puts the inner Lindblad resonance at 2.6 kpc and corotation at 10.1 kpc. For the density contrast (the amplitude of the density perturbation in the gas) I assumed 0.75. A good fit could be obtained using a logarithmic spiral with a pitch angle of 15^{o}, and invoking a phaseshift of 20^{o} between the maximum of the HI surface density and the potential minimum.

Fig. 9^{a} shows the "observed" residual velocities along the minor axis, averaged over its western and eastern halves (allowing for the sign reversal) as dots. The full drawn curve represents the linear density-wave model, i.e. the line-of-sight component of the radial motions. Fig. 9^{b} shows the same for the major axis and the tangential motions.

The agreement between the theoretical and observed velocities is good for the radial component of the density-wave streaming. For the tangential component it is much less pronounced. This may be caused, however, by the assumed rotation curve, since it is difficult to separate circular motions and non-circular tangential motions, whereas the separation of circular and radial motions (along the minor axis) is trivial and beyond question.

Non-linear effects and the phase shift which had to be invoked, as well as the conditions around the resonances should be considered in a more detailed study. We may conclude that density-wave theory is consistent with the present observations if the phase shift can be explained.

The Westerbork Radio Observatory is operated by the Netherlands Foundation for Radio Astronomy with financial support from the Netherlands Organization for the Advancement of Pure Research (Z.W.O.).

References:

Brandt, J.C., Kalinowski, J.K., Roosen, R.G. 1972, Astrophys. J. Suppl. 24, 421
Burton, W.B. 1971, Astron. and Astrophys. 10, 76
Lin, C.C., Yuan, C., Shu, F.H. 1969, Astrophys. J. 155, 721
Roberts, M.S. 1972, IAU Symp. No 44, Ed. D.E. Evans, p. 12
Rogstad, D.H. 1971, Astron. and Astrophys. 13, 108.
Rots, A.H. 1974, Dissertation, Groningen University
Shu, F.H. Stachnik, R.V., Yost, J.C. 1971, Astrophys. J. 166, 465
Tammann, G.A., Sandage, A.R. 1968, Astrophys. J. 151, 825

Figure Captions

Fig. 1. Radiograph of the density distribution of HI in M81. The half power beam width (FWHP) is shown in the lower right hand corner which contains also an indication of the linear scale in the plane of the galaxy; 64" corresponds to 1 kpc. The coordinates are right ascension and declination (1959.0). The thin features which look like pieces of large circles in the north-eastern quadrant of the figure are due to uncancelled parts of grating rings related to M82, and are thus spurious. The crosses indicate star positions and the center of M81. (Photo by University of Princeton Observatory).

Fig. 2. A contour map of the density distribution of HI superimposed on a 48-inch Schmidt photograph. The dashed, full, and thick contours correspond to column densities of 5, 10 and 20 x 10^{20} atom/cm^{2}, respectively. (Photo by Hale Observatories).

Fig. 3. Contour map of approximate surface density of HI (= observed column density times cos 59°) deprojected to a face-on orientation of the plane of M81. Note that this figure does not display the true surface density in the plane of the galaxy, since there is no information on the HI distribution along the line of sight. The contour interval is 1.6 $M_\odot/pc^2$; different shading begins at 3.2, 4.8 and 6.4 $M_\odot/pc^2$. Superimposed is a two armed logarithmic spiral with a pitch angle of 15°. The dashed circles have radii of 2.6 and 10.1 kpc. The line of nodes has the same orientation as in Figs. 1 and 2.

Fig. 4. HI surface density as a function of spiral phase (with respect to the eastern spiral arm). The surface density has been averaged over (logarithmic) spiral sectors 2° wide in spiral phase and stretching over 2 kpc in radius. The three panels show different radius ranges.

Fig. 5. B-V color as a function of spiral phase. The color index has been averaged over sectors 4° wide in spiral phase and extending from 4 to 6 kpc radius. It can be directly compared with the upper panel in Fig. 4.

Fig. 6. Lines of equal line-of-sight velocity superimposed on a 200-inch photograph. The contours are labeled by their heliocentric velocities (km/s). The coordinates are right ascension and declination (1950.0). Dashed lines connect the contours over areas where the signal-to-noise ratio is poor. (Photo by Hale Observatories).

Fig. 7. Rotation curve derived for M81. Within 3.5 kpc there is not enough HI to define the curve reliably. Between 3 and 10 kpc the northern and southern halves agree reasonably well. The full curve corresponds to the mass model in Fig. 8.

Fig. 8. Surface densities of matter, and of blue and yellow luminosities (Brandt et al., 1972) as functions of radius in the galaxy.

Fig. 9. Observed residual velocities (dots) and line-of-sight components of theoretical density-wave motions (drawn in full). a) Along the minor axis. b) Along the major axis. The data have been averaged over both halves of the axes (allowing for the sign reversal), since in both cases there is close agreement between the two halves. The signs of the velocities shown in this figure are correct for the western and northern halves of the axes. The abcissa is R, the distance to the center in the plane of the galaxy.

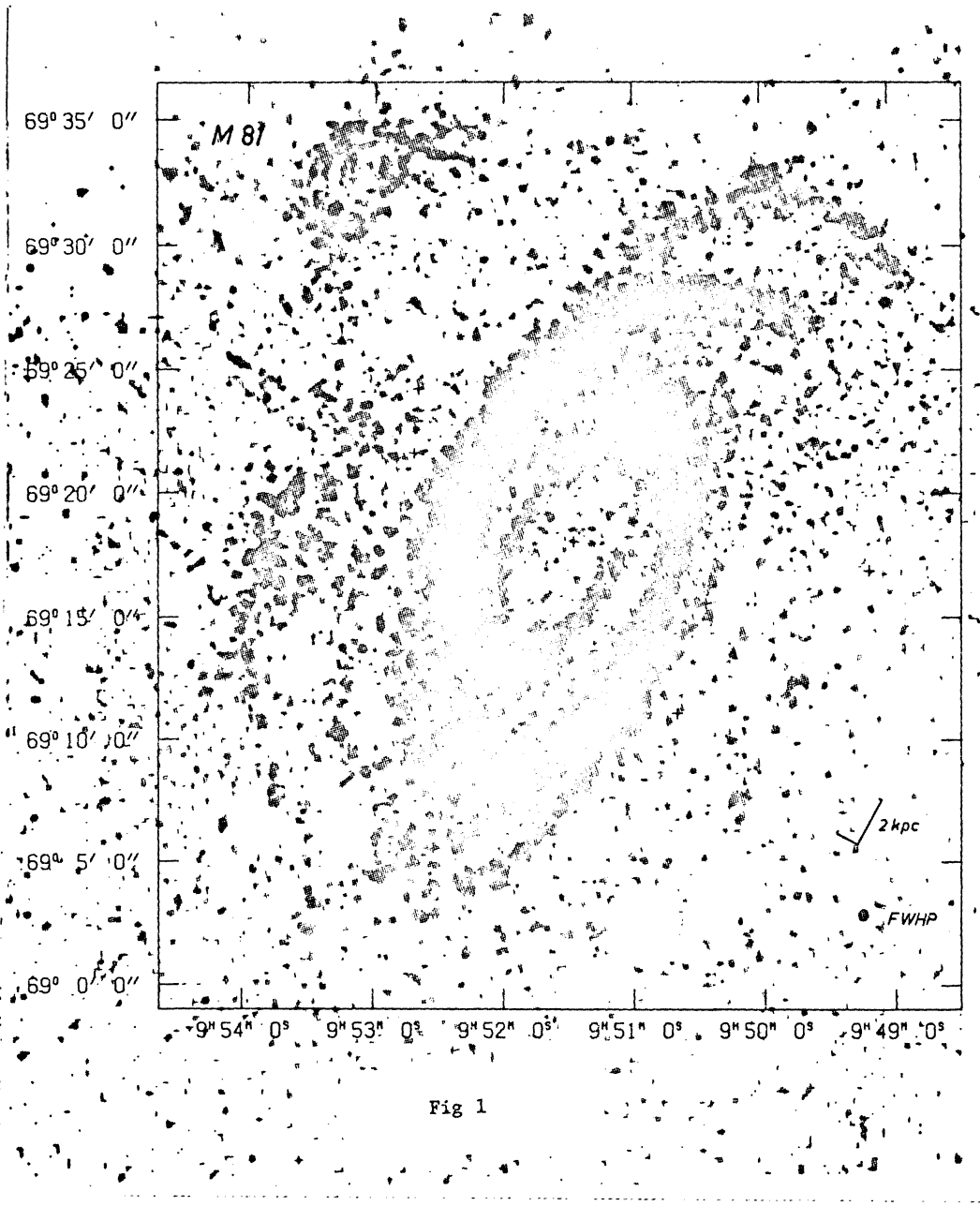
M 81
69° 35′ 0″
69° 30′ 0″
69° 25′ 0″
69° 20′ 0″
69° 15′ 0″
69° 10′ 0″
69° 5′ 0″
69° 0′ 0″
9H 54M 0S
9H 53M 0S
9H 52M 0S
9H 51M 0S
9H 50M 0S
9H 49M 0S
2 kpc
FWHP

Fig 1

Fig 2

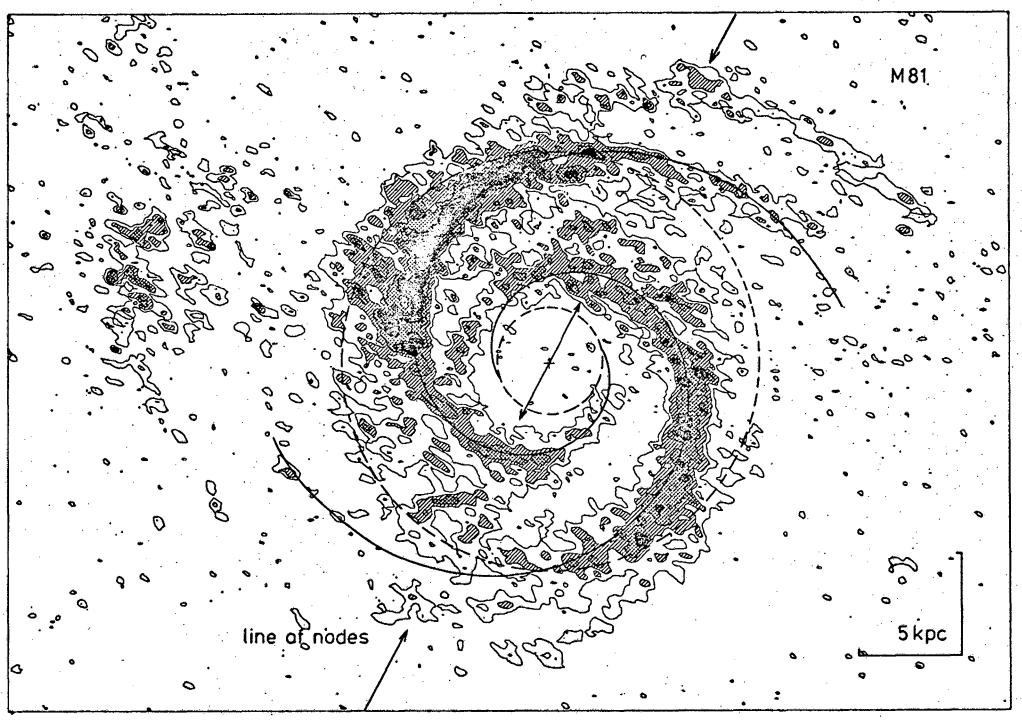
M81
line of nodes
5 kpc

Fig 3

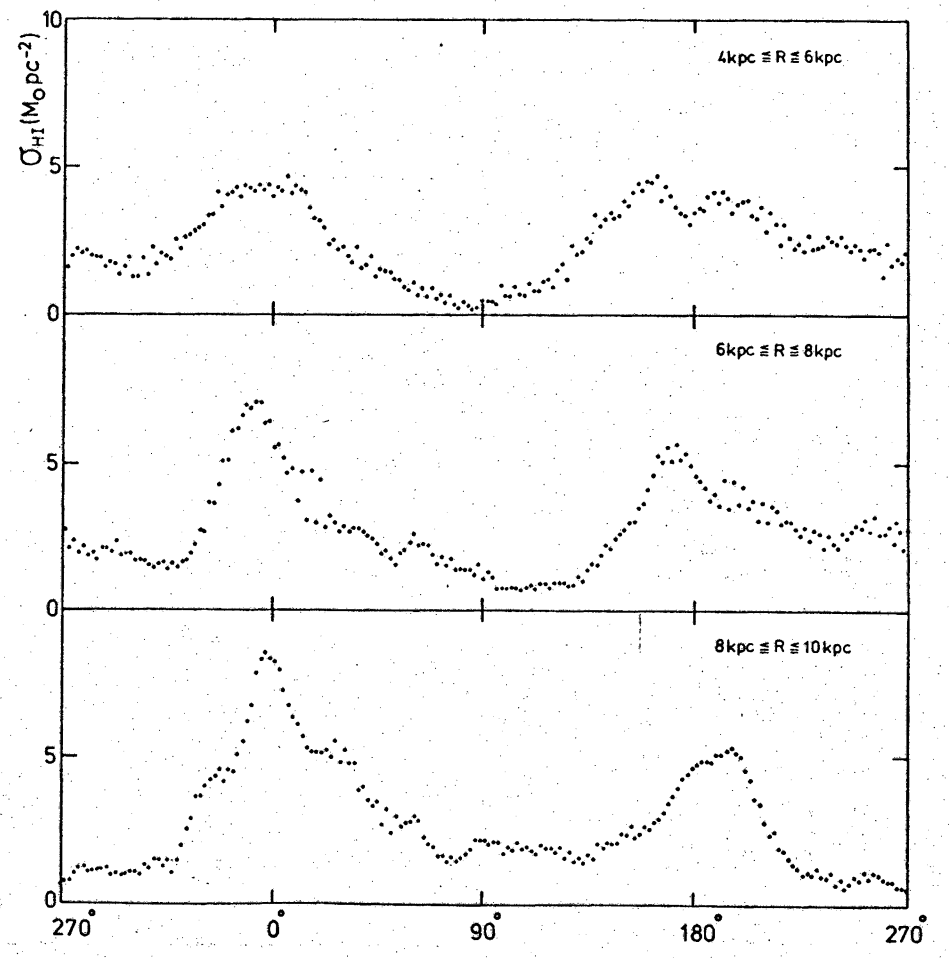
$\sigma_{HI}(M_\odot pc^{-2})$
10
5
0
4kpc ≅ R ≅ 6kpc
6kpc ≅ R ≅ 8kpc
8kpc ≅ R ≅ 10kpc
270°
0°
90°
180°
270°

Fig 4

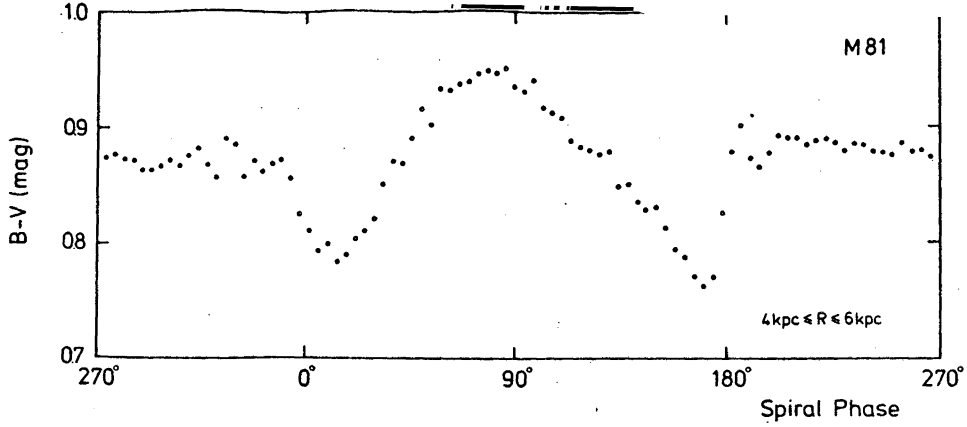

Fig 5

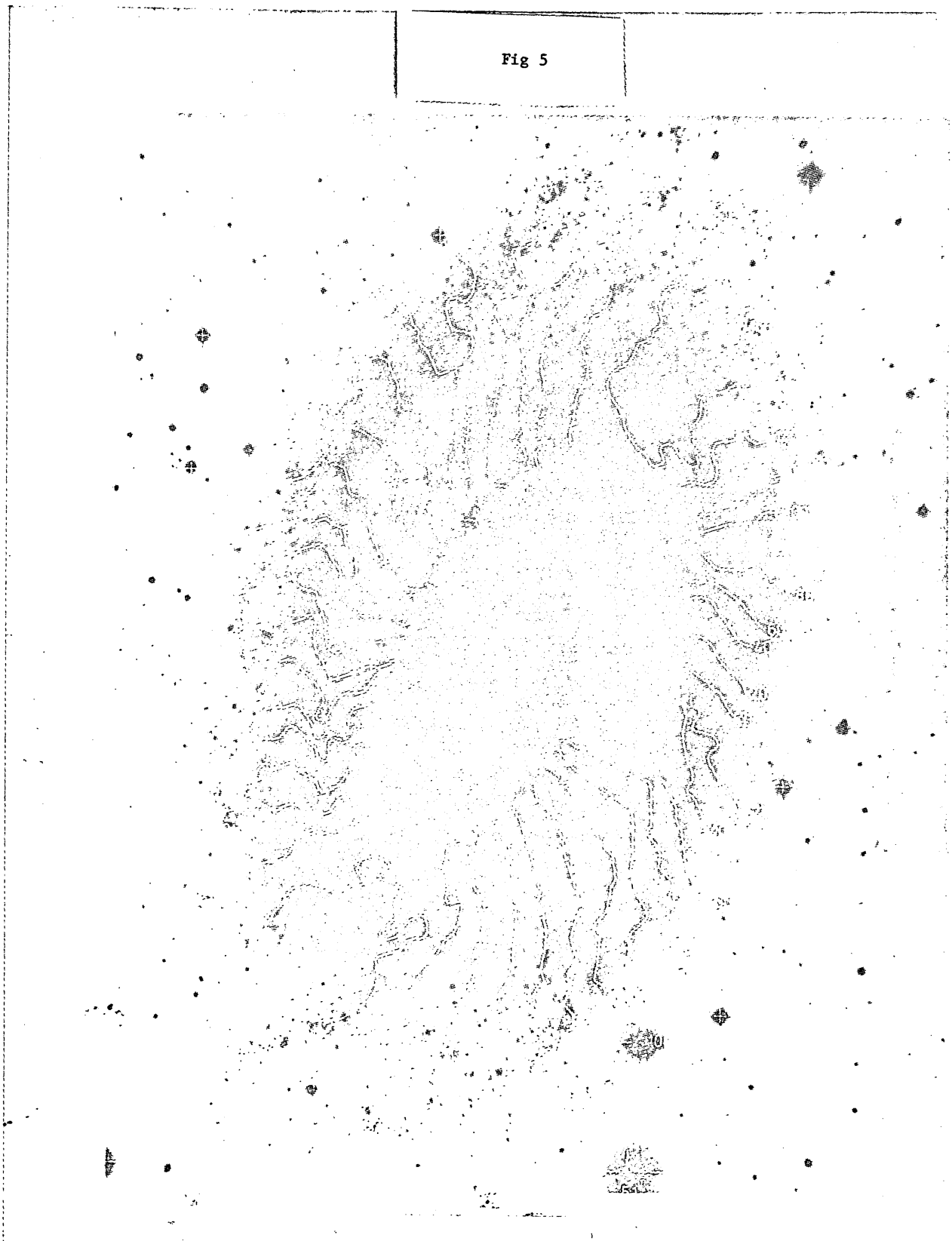

Fig 6

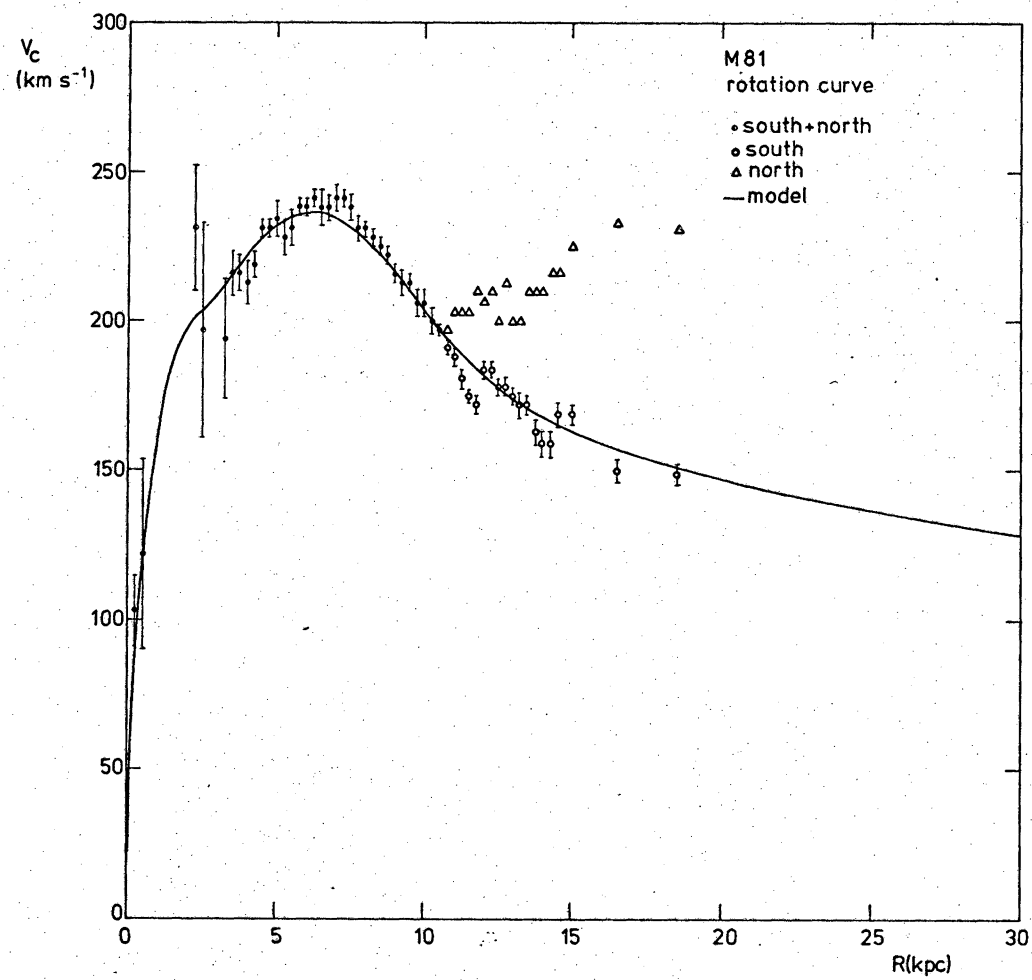
V_c
(km s^{-1})
M 81
rotation curve
south+north
south
north
model
300
250
200
150
100
50
0
0
5
10
15
20
25
30
R(kpc)

Fig 7

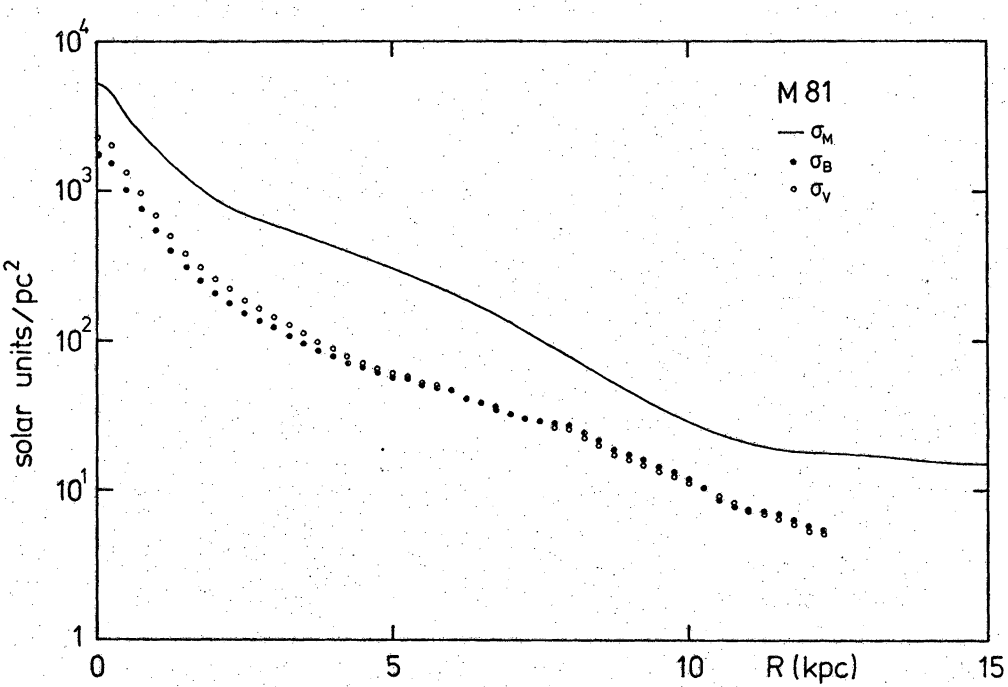
M 81
σ_M
σ_B
σ_V
10^4
10^3
10^2
10^1
1
solar units/pc^2
0
5
10
R (kpc)
15

Fig 8

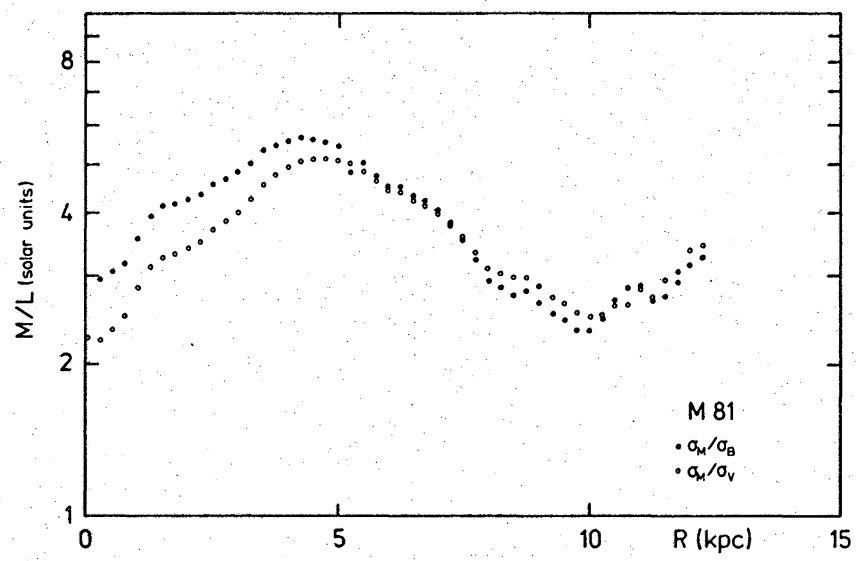

Fig 8[a]

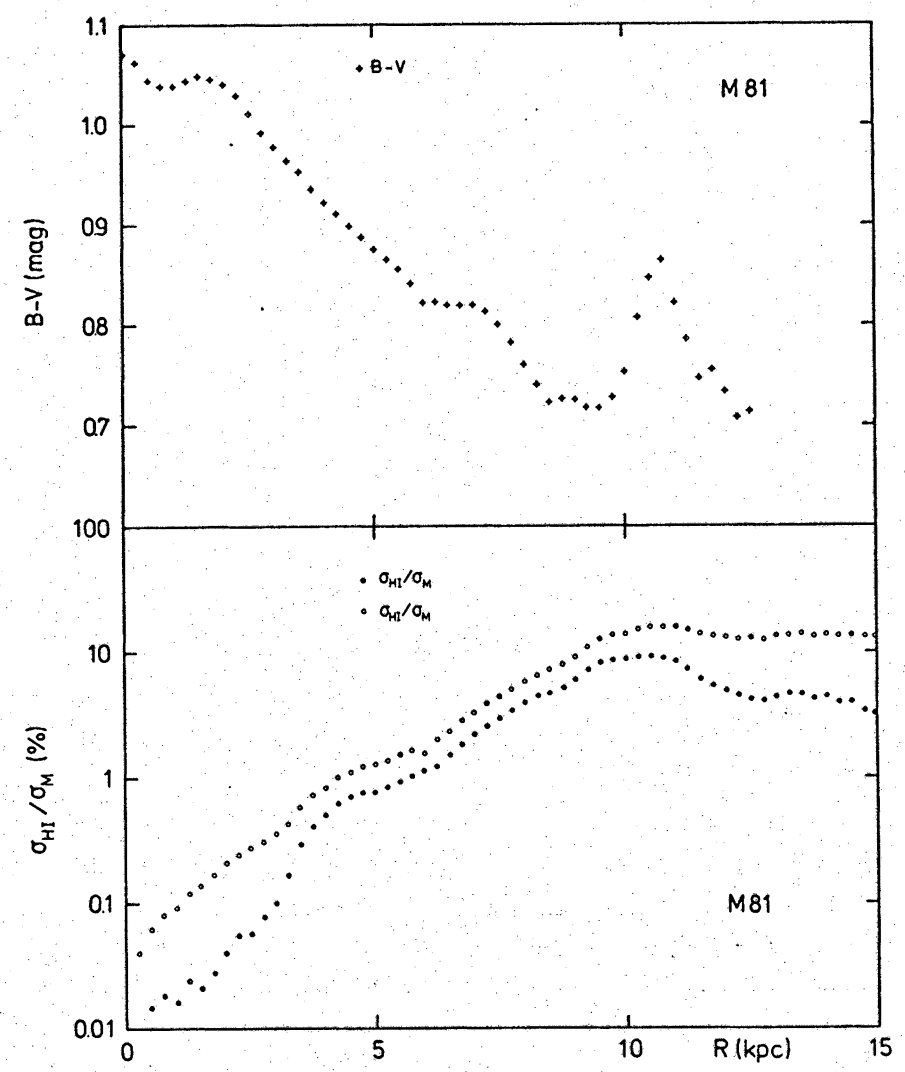

Fig 8[b]

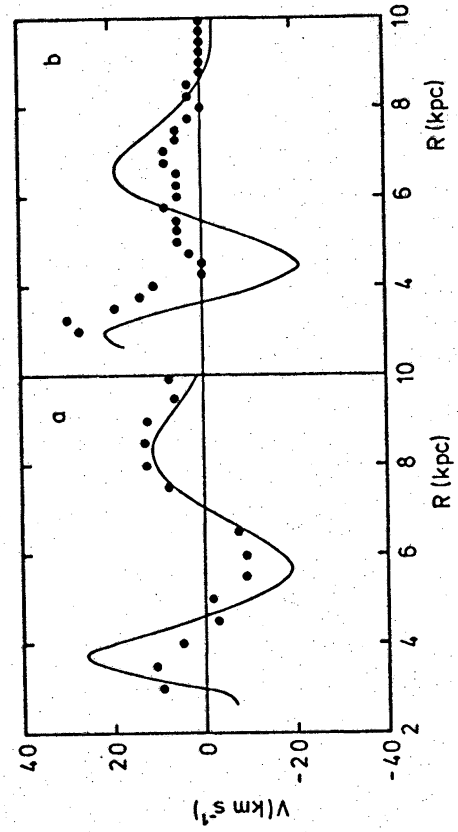

Fig 9